

Journal of Materials Chemistry B

Accepted Manuscript



This is an *Accepted Manuscript*, which has been through the Royal Society of Chemistry peer review process and has been accepted for publication.

Accepted Manuscripts are published online shortly after acceptance, before technical editing, formatting and proof reading. Using this free service, authors can make their results available to the community, in citable form, before we publish the edited article. We will replace this *Accepted Manuscript* with the edited and formatted *Advance Article* as soon as it is available.

You can find more information about *Accepted Manuscripts* in the [Information for Authors](#).

Please note that technical editing may introduce minor changes to the text and/or graphics, which may alter content. The journal's standard [Terms & Conditions](#) and the [Ethical guidelines](#) still apply. In no event shall the Royal Society of Chemistry be held responsible for any errors or omissions in this *Accepted Manuscript* or any consequences arising from the use of any information it contains.

Cite this: DOI: 10.1039/c0xx00000x

ARTICLE TYPE

www.rsc.org/xxxxxx

Poly(phenyleneethynylenes) nanoparticles: preparation, living cell imaging and potential application as drug carriers

Tong Chen,^{b‡} Wanfu Xu,^{c‡} Zehai Huang,^b Hongmei Peng,^b Zhiyong Ke,^{*c} Xinwei Lu,^a Yichen Yan^a and Ruiyuan Liu^{*a}

⁵ Received (in XXX, XXX) Xth XXXXXXXXXX 20XX, Accepted Xth XXXXXXXXXX 20XX

DOI: 10.1039/b000000x

Conjugated polymer nanoparticles (PPEs nanoparticles) are fabricated by self-assembly of a novel amphiphilic poly(phenyleneethynylenes). The morphology and cytotoxicity of PPEs nanoparticles were investigated. Moreover, confocal fluorescence microscopy and flow cytometry assay revealed the effective internalization of PPEs nanoparticles. PPEs nanoparticles were also used as a carrier for drug delivery system. Upon encapsulating an anticancer drug, DOX, PPEs nanoparticles exhibited high drug loading efficiency (26.6 wt%) and good release properties. Subsequently, DOX loaded PPEs nanoparticles were investigated by employing dynamic light scattering and transmission electron microscopy. Finally, cell uptake, cytotoxicity and Western blotting were carried out, which revealed that PPEs nanoparticles successfully deliver drug into cancer cells and keep the anticancer bioactivity of DOX. All these results indicated that this new type of PPEs nanoparticles would be a promising drug delivery system for therapeutic delivery and/or bioimaging applications.

Introduction

Chemotherapy has become an important cancer treatment due to its effective cancer cells killing potential. The major disadvantages of chemotherapeutic drugs is poor solubility, severe toxicity, high dosage, nonspecific delivery, and short circulating half-lives.¹ To overcome these shortcoming of conventional chemotherapy, polymeric nanoparticles have been utilized as drug delivery vehicles based on their unique properties, such as higher bioavailability of the drug in the tumour owing to an enhanced permeation and retention (EPR) effect, controlled release of the drug, longer circulation times, and overcoming multidrug resistance.² Over the past few decades, a series of polymeric nanoparticles have been exploited as chemotherapeutic drug delivery carriers, and they are generally formed by self-assembly of amphiphilic polymers in aqueous solution while the hydrophobic drug is loaded in the hydrophobic core of nanoparticles.³

However, there are still some disadvantages by using polymeric nanoparticles in therapeutic applications. For example, the process of drug released from polymeric nanoparticles cannot be tracked because no specific signals can be captured.⁴ On the other hand, the integration of fluorescent signal reporters with drug into polymeric nanoparticles can provide an approach to simultaneously intracellular trace and therapy which benefit the treatment and study of cancer. Recently, small fluorescent dyes and quantum dots have been employed to integrate into polymeric nanoparticles for cellular imaging which make the possibility of real time tracking of therapy agents and visualizing the therapeutic effects *in vitro* and

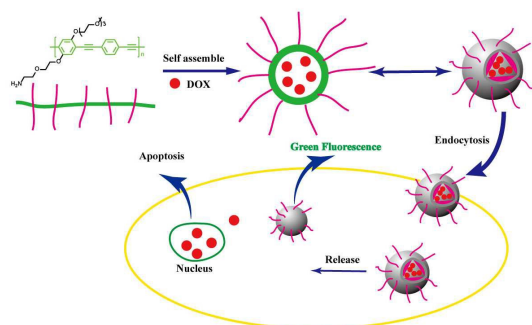
in vivo.⁵ However, poor photostability of small fluorescent dyes and inherent toxicity of quantum dots limit their broad applicability.

Therefore, new fluorescent materials with improved properties (nontoxicity, highly fluorescent, photostable, good biocompatible and minimal perturbation to biological systems) are in high demand. Among them, poly(phenyleneethynylenes) (PPEs) seem to be interesting candidates due to their unique properties. PPEs are conjugated polymers which contain delocalized π -electron main chain, exhibit high fluorescence quantum yield, large extinction coefficients, photostability, and efficient optical signal transduction.⁶ In addition, the synthetic versatility of PPEs allows a wide selection of functional side groups such as triethylene glycol monomethyl ether groups, sugars, carboxyl group, thioureas, 2-thiohydantoin, amino and DNA.⁷ Given these properties, PPEs have attracted much attention in biomedical applications involving in bioimaging, biomolecules detection, and gene delivery.⁸

In this work, we design and synthesize diiodobenzene derivative **1**, which contains hydrophilic groups such as amino group and triethylene glycol monomethyl ether group (Scheme 2), and polymerize it with *para*-diethynylbenzene to obtain the corresponding amphiphilic PPEs [poly(**1**)]. It is anticipated that poly(**1**) will self assemble to fabricate poly(phenyleneethynylenes) nanoparticles (denoted PPEs nanoparticles). The chemical composition and structures of poly(**1**) were fully characterized. The morphology and cytotoxicity of PPEs nanoparticles were investigated. To further explore their potential biomedical applications, the biocompatibility, cell uptake behaviour and bioimaging of PPEs

nanoparticles were further evaluated. Our results showed that PPEs nanoparticles could be a fluorescent reporter for cellular imaging.

In addition, DOX was chosen as the model drugs, to explore the potential applications of PPEs nanoparticles as drug carriers. *In vitro* drug release studies were carried out at pH 7.4 (physiological pH) and pH 5.5 (endolysosomal pH). The morphology of DOX loaded PPEs nanoparticles were investigated. Cellular uptake, cytotoxicity and apoptosis studies of DOX loaded PPEs nanoparticles were also performed. Our experiments indicated that PPEs nanoparticles could deliver drugs into cancer cells and keep the anticancer bioactivity of DOX (scheme 1).



Scheme 1 Schematic illustration of the formation of DOX loaded PPEs nanoparticles, as well as the release of payloads in cell.

Experimental

Materials

For use as polymerization solvents, DMF and Et₃N were distilled over CaH₂. *para*-Diethynylene benzene, Pd(Ph₃)₂Cl₂, CuI, PPh₃, doxorubicin (DOX) were purchased from Sigma-Aldrich. All other reagents were commercially obtained and used without further purification. Deionized (DI) water produced by Milli-Q water purification system and has a resistivity of 17.9 mΩ/cm. 2,5-Diiodobenzene-1,4-diol was synthesized according to reference 9. 2-(2-(2-Methoxyethoxy)ethoxy)ethyl 4-methylbenzenesulfonate was prepared according to reference 10. 2-(2-((*tert*-Butoxycarbonyl)amino)ethoxy)ethyl 4-methylbenzenesulfonate was synthesized according to reference 11.

Characterization.

¹H (400 MHz) and ¹³C (100 MHz) NMR spectra were recorded on a Bruker Avance/DMX 400MHz NMR spectrometer with DMSO-*d*₆ and tetramethylsilane as an internal reference. IR spectra were measured using a Shimadzu FTIR-8100 spectrophotometer. The melting points (mp) were determined on a Yanaco micro-melting point apparatus and elemental analysis was performed on an Eager 300 elemental microanalyzer. UV-vis spectra were recorded in a quartz cell (thickness: 1 cm) at room temperature using a JASCO J-820 spectrophotometer. Fluorescence spectra were obtained using a FluoroMax-4 spectrofluorometer with a xenon lamp and 1.0cm quartz cells. The number- and weight-average molecular weights (*M*_n and *M*_w, respectively) of the polymer were determined using gel permeation chromatography (GPC) on a Jasco Gulliver system (PU-980, CO-965, RI-930, and UV-1570) equipped with polystyrene gel columns (Shodex columns K804, K805, and

J806) and calibrated by polystyrene standards at 40 °C using THF as the eluent.

Synthesis of Diiodo Benzene Derivatives (1).

2,5-Diiodohydroquinone (10.83 g, 30 mmol), K₂CO₃(8.28 g, 60 mmol), and 2-(2-(2-methoxyethoxy)ethoxy)ethyl 4-methylbenzenesulfonate (6.36 g, 20 mmol) were dissolved in CH₃CN, and the mixture was refluxed for 48 h. The mixture was then filtered, followed by concentration of the filtrate using a rotary evaporator. The residue was purified via silica gel column chromatography with *n*-hexane/AcOEt(1:2, v/v) as the eluent to obtain diiodobenzene derivative **b** as a pale gray powder in 80% yield (8.07g, 15.9 mmol).

Diiodobenzene derivative **b** (5.08 g, 10 mmol), K₂CO₃ (2.76 g, 20 mmol), and 2-(2-((*tert*-butoxycarbonyl)amino)ethoxy)ethyl 4-methylbenzenesulfonate (3.59 g, 10 mmol) were dissolved in CH₃CN, and the mixture was refluxed for 48 h. The mixture was then filtered, followed by concentration of the filtrate using a rotary evaporator. The residue was purified via silica gel column chromatography with *n*-hexane/AcOEt(1:4, v/v) as the eluent to obtain diiodobenzene derivative **c** as a pale gray powder in 89% yield (6.18 g, 8.9 mmol).

Diiodobenzene derivative **c** (5.56g, 8 mmol) was dissolved in CH₂Cl₂/CF₃COOH(1/1, v/v), and the mixture was stirred at room temperature overnight. The mixture was concentrated on a rotary evaporator. The residue was dissolved in CH₂Cl₂. The organic layer was washed with saturated aqueous NaHCO₃, and evaporated to dryness. The crude product was recrystallized in MeOH to obtain monomer **1** in 97% yield (4.62 g, 7.76 mmol).

Mp 175~176.5 °C,

¹H NMR (400 MHz, DMSO-*d*₆) δ 10.10(s, 1H), 7.28 (s, 1H), 7.24(s, 1H), 4.05(s, 2H), 3.73(s, 2H), 3.67~3.59 (d, J=4.5Hz, 2H), 3.58~3.47(dd, J=8.8, 4.4Hz, 4H), 3.46~3.30 (m, 13H).

¹³C NMR (100 MHz, DMSO-*d*₆) δ 151.98, 151.16, 123.85, 122.91, 86.93, 84.17, 71.26, 70.14, 69.85, 69.77, 69.61, 68.98, 58.05, 40.11, 39.90, 39.69, 39.48, 39.28, 39.07, 38.86.

IR (KBr, cm⁻¹): 3372, 3103, 2907, 1725, 1582, 1444, 1361, 1243, 1101, 1015, 908, 827, 801, 687.

Anal. Calcd for C₁₇H₂₇I₂NO₆: C, 34.30; H, 4.57; N, 2.35.

Found: C, 34.15; H, 4.62; N, 2.44.

Synthesis of Poly(phenyleneethynyls).

All polymerizations were performed in a glass tube equipped with a three-way stopcock under nitrogen. A representative experimental procedure for the polymerization of **1** with *para*-diethynylbenzene is given below.

A solution of **1** (595 mg, 1.00 mmol), *para*-diethynylbenzene (126 mg, 1.00 mmol), PdCl₂(PPh₃)₂ (35 mg, 50 μmol), CuI (4.7 mg, 25 μmol), PPh₃ (26.2 mg, 100 μmol), and Et₃N (2.00 mL, 14.3 mmol) in DMF (3.00 mL) was stirred at 60 °C for 24 h. The resulting mixture was poured into MeOH/acetone [4:1v/v, 300 mL] to effect precipitation of the formed polymer, which was separated by filtration using a membrane filter (ADVANTEC H100A047A) and dried under reduced pressure.

Poly(**1**): GPC (THF, polystyrene standard): *M*_w=35108, *M*_n=13400, PDI=2.62.

¹H NMR (400MHz, DMSO-*d*₆, ppm): δ 7.69~7.38 (m, 4H, Ar), 7.01~6.86 (m, 2H, Ar), 4.15~4.09 (d, 2H), 3.87~3.76 (d, 4H), 3.59~3.46(m, 6H), 3.30~3.25 (m, 11H).

IR (KBr, cm⁻¹): 3548, 3157, 2943, 2278, 1655, 1602, 1503, 1461, 1431, 1412, 1312, 1266, 1168, 1010, 830, 741, 690, 518.

Preparation and Characterization of Poly(phenyleneethynylene)s Nanoparticles (PPEs Nanoparticles)

Preparation of PPEs Nanoparticles

PPEs nanoparticles were prepared via dialysis method. Briefly, 10 mg poly(1) were first dissolved in 10 mL DMSO. The mixture was stirred for 2 h at room temperature. 5 mL of DI water was then drop-wise under magnetic stirring. The mixture was placed into a dialysis bag (MWCO = 3500) and dialyzed against DI water for 24 h to remove DMSO. After that, the solution was frozen and lyophilized.

Characterization of PPEs Nanoparticles

Prepared PPEs nanoparticles were characterized using dynamic light scattering (DLS) (Zetasizer Nano ZS, Malvern Instruments Ltd., UK) and transmission electron microscope ([TEM] H-7650; HITACHI, Tokyo, Japan) operating at 200 kV.

Dynamic light scattering (DLS) measurements were carried out operating at a wavelength of 632.8 nm and a 173° detection angle equipped with a Peltier temperature control unit. The hydrodynamic radius of nanoparticles was determined with a Laplace inversion program (CONTIN).

TEM samples were prepared by dripping PPEs nanoparticles solution onto a copper grid cover with carbon. The solvent was gently absorbed away by a filter paper. The grids were then allowed to dry in air at room temperature before observation.

Cytotoxicity of PPEs Nanoparticles

Cell Culture

PC3 cells were obtained from American Type Culture Collection and cultured according to the manufacturer's recommendations.

Cytotoxicity of PPEs Nanoparticles

The cell viability of PPEs nanoparticles on PC3 cells was evaluated by cell counting kit-8 (CCK-8) assay. Briefly, cells were seeded in 96-well microplates at a density of 5×10^4 cells/mL in 160 μ L of media containing 10% FBS. After 24 h of cell attachment, the cells were incubated with PPEs nanoparticles for 24 h. Then PPEs nanoparticles were removed and cells were washed with PBS three times. 10 μ L of CCK-8 dye and 100 μ L of DMEM cell culture medium were added to each well and incubated for 2 h at 37 °C. Plates were then analyzed with a microplate reader (Victor, Perkin-Elmer) at 450 nm.

Measurements of formazan dye absorbance were carried out at 450 nm, with the reference wavelength at 620 nm. The values were proportional to the number of live cells. The percent reduction of CCK-8 dye was compared to controls (cells not exposed to PPEs nanoparticles), which represented 100% CCK-8 reduction. Three replicate wells were used per microplate, and the experiment was repeated three times. Cell survival was expressed as absorbance relative to that of untreated controls. Results are presented as mean standard deviation (SD).

Confocal Microscopic Imaging of Cells Incubated with PPEs Nanoparticles

To visualize the cellular uptake of PPEs nanoparticles, confocal laser scanning microscopy was employed. PC3 cells were seeded in Petri plates with a glass bottom at a density of 1×10^4 cells/plate, and the plates were incubated at 37 °C for 24 h in a CO₂ incubator. Cells were incubated with PPEs nanoparticles at a final concentration of 50 μ g/mL for 12 h at 37 °C. Afterward, the cells were rinsed three times with PBS to remove excess PPEs nanoparticles. Cells were then stained with 150 μ L of DAPI for 30 min with intermediate washing with PBS and observed under

the confocal laser scanning microscope (Olympus IX81 with DU897 mode). Images were obtained at 100 \times magnification from the fluorescence emitted by PPEs nanoparticles (460 nm) and DAPI (505 nm).

Flow Cytometry Analysis

PC3 cells were seeded in 24-well plates at a density of 1×10^4 cells per well and cultured with 1 mL of DMEM containing 10% FBS for 24 h. PPEs nanoparticles were added to the plates (at 50 μ g/mL). After 12 hours of treatment, the medium was discarded and the cells were washed three times with PBS. All the cells were digested by trypsin and collected in centrifuge tubes for centrifugation at 1000 rpm for 5 min. The supernatant was discarded and the bottom cells were washed twice with PBS. The suspended cells were then filtered and examined by flow cytometry (BD FACSAria™ III, USA). The instrument was calibrated with non-treated cells (negative control) to identify viable cells, and the cells were determined from a fluorescence scan performed with 1×10^4 cells using the FL1-H channel.

Preparation and Characterization of DOX Loaded PPEs Nanoparticles

Preparation of DOX Loaded PPEs Nanoparticles

In Vitro DOX was loaded into PPEs nanoparticles during the nanoparticles formation. Briefly, 10 mg poly(1) were dissolved in 10 mL DMSO containing 3 mg DOX. Then, 5 mL DI water was added dropwise to the mixture, followed by dialysis against DI water for 48 h at room temperature (MWCO = 3500) to remove the unloaded drugs and DMSO. After that, the solution was frozen and lyophilized.

Characterization of DOX Loaded PPEs Nanoparticles

Prepared DOX loaded PPEs nanoparticles were characterized using dynamic light scattering (DLS) (Zetasizer Nano ZS, Malvern Instruments Ltd., UK) and transmission electron microscope ([TEM] H-7650; HITACHI, Tokyo, Japan) operating at 200 kV.

The amount of DOX was determined using a UV-vis JASCO J-820 spectrophotometer at 485nm. For determination of drug loading content, lyophilized DOX loaded PPEs nanoparticles were dissolved in DMSO and analyzed with UV spectroscopy, wherein the calibration curve was obtained with DOX in DMSO solutions with different DOX concentrations. Drug loading content (DLC) and drug loading efficiency (DLE) were calculated according to the following formula:

$$\text{DLC}(\text{wt}\%) = (\text{weight of loaded drug} / \text{weight of polymer}) \times 100\%$$

$$\text{DLE}(\text{wt}\%) = (\text{weight of loaded drug} / \text{weight of drug in feed}) \times 100\%$$

The cell viability of DOX loaded PPEs nanoparticles on PC3 cells was evaluated by cell counting kit-8 (CCK-8) assay.

In Vitro Release of DOX from DOX Loaded PPEs Nanoparticles

The release profiles of DOX loaded PPEs nanoparticles were studied using a dialysis tube (MWCO = 3500) at 37 °C in pH 7.4 or 5.5 PBS. Briefly, 5mg DOX loaded PPEs nanoparticles were added into a dialysis tube. Then, the dialysis tube was put into a centrifuge tube with 20 mL PBS. At predetermined time intervals, 2 mL aliquots of the aqueous solution were withdrawn from the release media and another 2 mL fresh PBS was added into the release media. The amount of DOX released was calculated by determining the DOX concentration in the external buffer using a UV spectrophotometer at 485 nm.

Intracellular Release of DOX from DOX Loaded PPEs Nanoparticles

The ability of PPEs nanoparticles to transport DOX into PC3 cells was assessed by confocal laser scanning microscopy. PC3 cells were seeded in Petri plates with a glass bottom at a density of 1×10^4 cells/plate, and the plates were incubated at 37 °C for 24 h in a CO₂ incubator. The DOX loaded PPEs nanoparticles (with a DOX dosage of 2.5 µg/mL) were added to the plate.

After co-incubation for 12 h, the medium was removed and the cells were washed with PBS three times. Cells were then stained with 150 µL of DAPI for 30 min with intermediate washing with PBS and observed under the confocal laser scanning microscope (Olympus IX81 with DU897 mode). Images were obtained at 100× magnification from the fluorescence emitted by PPEs nanoparticles (460 nm), DAPI (505 nm), and DOX (560 nm).

Western Blotting Analysis

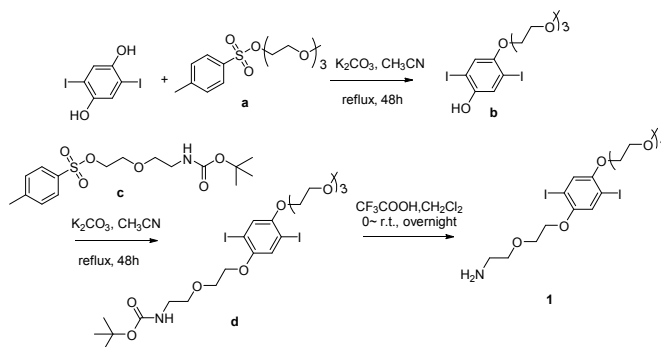
All the cell apoptosis in PC3 cells was evaluated by Western Blotting analysis. A representative experimental procedure for the DOX loaded PPEs nanoparticles is given below.

PC3 cells were seeded in two 6-well plates with 1×10^5 cells in 2 mL of DMEM medium per well. After attachment, the medium was replaced fresh medium containing DOX loaded PPEs nanoparticles solution. The remaining well of the plate was set as a control without any treatment. The final concentration of DOX is 2.5 µM in 2 mL culture medium of each well. After 24 h of incubation, DOX loaded PPEs nanoparticles solution was replaced with the fresh medium for another 60 h. After that, cells in each well were washed with cold PBS and lysed with a cell lysis buffer. Protein was extracted with $2 \times$ SDS sample buffer at 100 °C for 10 min and analyzed by immunoblotting to detect as indicated antibody. Briefly, the proteins were separated by gel electrophoresis on a 10% polyacrylamide gel containing SDS and then were blotted onto a polyvinylidenedifluoride (PVDF) membrane according to a standard protocol. After blocking in 5% milk in phosphate buffer saline tween 20 (PBST) for 1 h at room temperature, the membrane was incubated with primary antibody (1 : 1000~1:2000) overnight at 4 °C. After being washed with PBST three times, the membrane was incubated with corresponding secondary antibody (1:2000) for 1 h at room temperature. After the PBST was washed again, the signal of the membrane was detected by enhanced chemiluminescence substrates (Perkin Elmer).

Statistical analysis

All statistical analyses and figures were completed using GraphPad Prism V software. The unpaired *t* test was used to determine the significance of differences in cell viability assay, A P value of less than 0.05 was considered statistically significant.

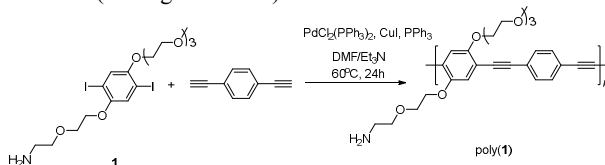
Result and Discussion



Scheme 2 synthesis of **1**

Synthesis and Characterization of Poly(phenyleneethynynes)

Diiodobenzene monomer **1** was synthesized using the route illustrated in Scheme 2. First, 2,5-dihydroxybenzene-1,4-diol was reacted consecutively with 2-(2-(2-methoxyethoxy)ethoxy)ethyl 4-methylbenzenesulfonate and 2-(2-((*tert*-butoxycarbonyl)amino)ethoxy)ethyl 4-methylbenzenesulfonate to afford corresponding diiodobenzene derivative **d**. Then, diiodobenzene derivative **d** was deprotected to afford diiodobenzene monomer **1**. The monomer was obtained as a pale gray powder and characterized by spectroscopic methods; satisfactory data corresponding to its molecular structure were obtained (see Figure S1–S3).



Scheme 3 Synthesis of poly(phenyleneethynynes) from **1** and *para*-diethynylbenzene

Sonogashira-Hagihara polycondensation of **1** with *para*-diethynylbenzene was carried out in DMF at 60 °C for 24 h (Scheme 3). The corresponding polymer [poly(**1**)] was obtained in 82 % yield with an *M_n* of 13400 and PDI of ~2.6. The structure of poly(**1**) was spectroscopically characterized (see Figure S4 and S5). The ¹H NMR and IR spectra of poly(**1**) exhibited signals that reasonably correlate with the structure illustrated in Scheme 3.

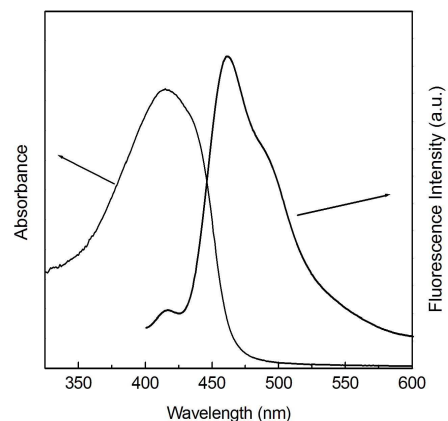


Figure 1 UV-vis and emission spectra of poly(**1**) in water

Figure 1 shows the absorption and emission spectra of poly(**1**) in water containing 10% DMSO. The absorption spectrum of poly(**1**) features a strong absorption band with a maximum at 410 nm, which is assigned to the $\pi \rightarrow \pi^*$ transition of the conjugated

polymer chains. The fluorescence spectra are structured with maximum intensity peaks at 470 nm.

Preparation and Characterization of PPEs Nanoparticles

In order to form the self-assembled nanoparticles, poly(**1**) was solubilised in DMSO and the DI water was added drop wise in the resulting solution, followed by dialysis against DI water.

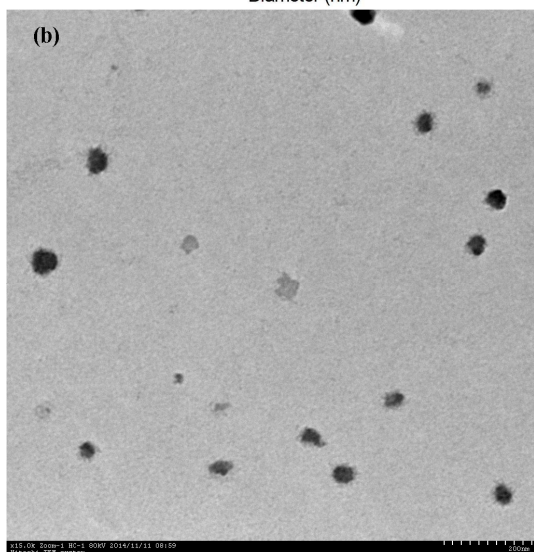
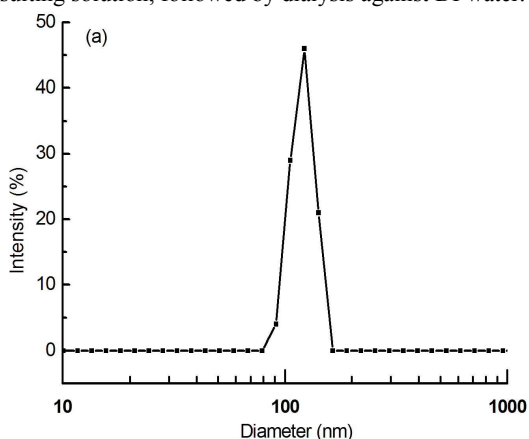


Figure 2 (a) Size distribution of PPEs nanoparticles as determined by DLS measurements, (b) Transmission electron micrographs of PPEs nanoparticles.

TEM and DLS measurements were used to investigate the morphologies and sizes of PPEs nanoparticles. As shown in Figure 2a, PPEs nanoparticles have an average hydrodynamic diameter of 117 nm determined by DLS analysis. According to Figure 2b, the sizes from TEM measurement are smaller than those from DLS analysis. This phenomenon may be due to the more extended hydrophilic side chains in water phase in DLS measurement, while they tend to collapse at the dry state.

Cytotoxicity of PPEs Nanoparticles.

The cytotoxicity of PPEs nanoparticles was evaluated in PC3 cells using the CCK-8 assay at concentration from 0–120 $\mu\text{g/mL}$ of PPEs nanoparticles for 24 h, respectively, and the results are shown in Figure 3. PPEs nanoparticles showed limited cytotoxicity. Around 80% of PC3 cells were still viable, when PPEs nanoparticles concentration reached 100 $\mu\text{g/mL}$.

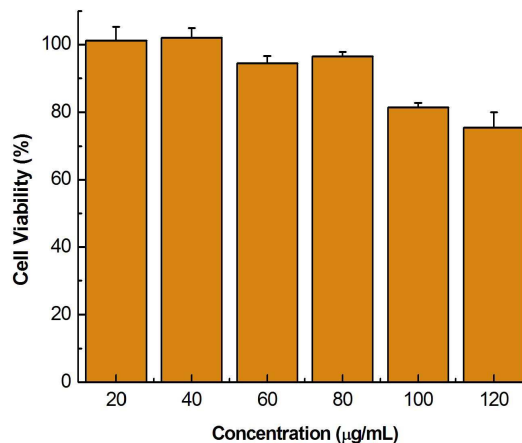


Figure 3 Cell viability of PC3 cells incubated with PPEs nanoparticles at various concentrations.

In Vitro Cell Image of PPEs Nanoparticles

We used PC3 cells as a model cell to study the subcellular distributions of PPEs nanoparticles by confocal laser scanning microscopy. The cell internalization study was carried out with PPEs nanoparticles concentration of 50 $\mu\text{g/mL}$. Cultured PC3 cells were incubated with PPEs nanoparticles for 12 h at 37 $^{\circ}\text{C}$. Then DAPI (10 $\mu\text{g/mL}$) was also used to co-stain the cells. As shown in Figure 4, PPEs with green fluorescence were cell membrane permeable and localized in the cytoplasm region. These results clearly showed that PPEs nanoparticles have good cell membrane permeability and good biocompatibility.

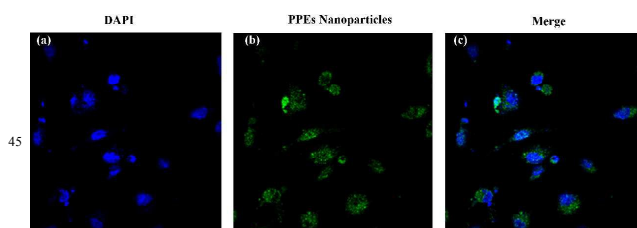


Figure 4 Fluorescence images of PC3 cells after incubation with PPEs nanoparticles for 12 h. For each panel, images from (a) were cells with nuclear staining with DAPI (blue), (b) cells with PPE-nanoparticles (green), (c) overlays of blue and green fluorescence channels.

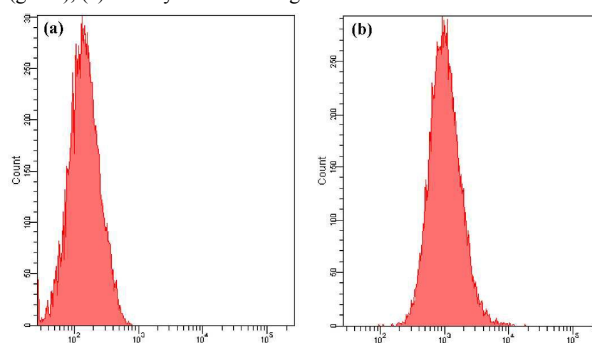


Figure 5 Flow cytometry profiles of PC3 cells that were incubated with PBS (a) or PPEs nanoparticles (b) at 37 $^{\circ}\text{C}$ for 12 h.

The flow cytometry analysis was also carried out to evaluate the cell internalization of PPEs nanoparticles by PC3 cells. PC3 cells without any treatment served as a blank control, showing only the autofluorescence originating from the cells (Figure 5a). PPEs nanoparticles were incubated with PC3 cells at 37 $^{\circ}\text{C}$ for 12 h. As shown in Figure 5, the relative geometrical mean

fluorescence intensity of cells pretreated with PPEs nanoparticles is almost 100-fold higher than that of non-pretreated cells, indicating PPEs nanoparticles can be easily internalized by PC3 cells. The cytometry examination agreed very well with the CLSM observation concerning the high cellular uptake of PPEs nanoparticles.

Drug Loading and *In vitro* Drug Release

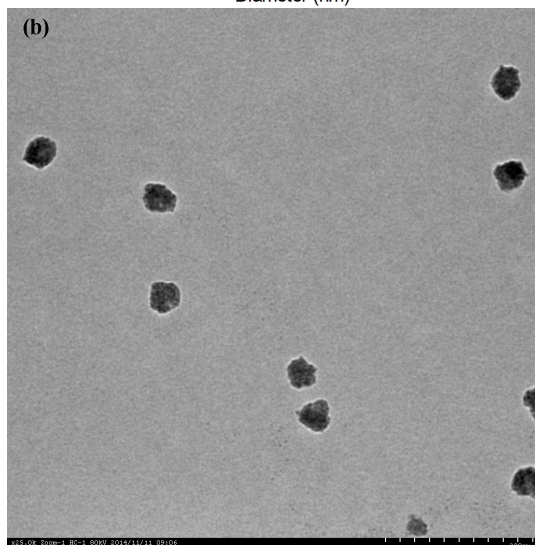
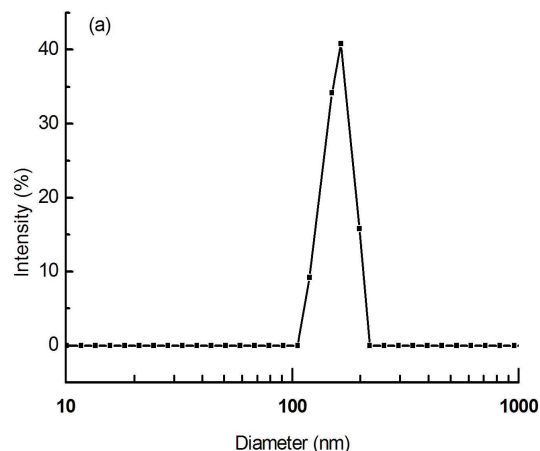


Figure 6(a) Transmission electron micrographs of DOX loaded PPEs nanoparticles (b) Size distribution of DOX loaded PPE nanoparticles as determined by DLS measurements.

DOX loading was performed by dropwise addition of DI water into DMSO solution of poly(I) and DOX followed by dialysis. DOX could be encapsulated into polymer nanoparticles self-assembled from amphiphilic polymer containing hydrophobic main chain and hydrophilic side groups due to the strong intermolecular interaction between DOX and polymer main chain¹². It seems that the π - π stacking interaction between PPEs main chain and DOX promote the loading of DOX into the PPEs nanoparticles. The loading capacity and efficiency of PPEs nanoparticles were measured to be 5.1% and 26.6%, respectively. Figure 6 shows TEM images and corresponding particle size distribution curve of DOX loaded PPEs nanoparticles, respectively. DLS measurement showed that the diameter of DOX loaded PPEs nanoparticles in aqueous solution increase to around 158 nm. Thus the loading of DOX did not change the nanoparticle size significantly.

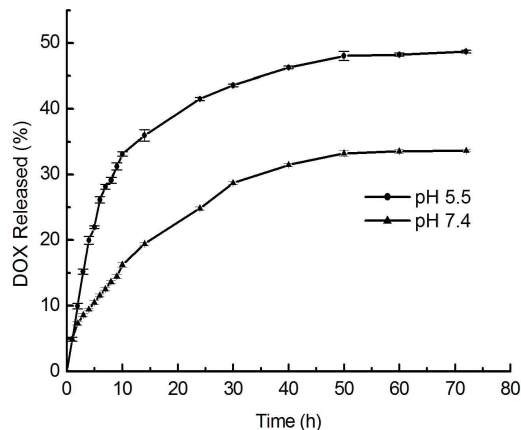


Figure 7 Release profiles of DOX from PPEs nanoparticles at 37 °C in pH 7.4 and pH 5.5 buffer solutions.

The release studies were carried out at 37 °C in different buffers (pH 5.5 and pH 7.4). As presented in Figure 7, the release is not obvious both in pH 5.5 and pH 7.4 conditions, and the release of DOX increases with the increasing time. At pH 7.4, DOX loaded PPEs nanoparticles showed a cumulative release of DOX about 33% after 50 h, while the value obviously increased to 48% in pH 5.0 medium at the same time. The release rates increased in PBS at pH 5.5 due to the improved solubility of protonized DOX in water.

Cytotoxicity and Cell Internalization Studies DOX Loaded PPEs Nanoparticles.

To evaluate the cell uptake of DOX loaded PPEs nanoparticles, confocal laser scanning microscopy observation was performed. DOX loaded PPEs nanoparticles were incubated with PC3 cells. The concentration of DOX in DOX loaded PPEs nanoparticles was kept at 2.5 $\mu\text{g/mL}$. As shown in Figure 8, the presence of DOX loaded PPEs nanoparticles in PC3 cells is observed by the red colour emitted from DOX in the nuclei and green colour emitted from PPEs in the cytoplasm after incubation for 12 h. These results indicated that DOX loaded PPEs nanoparticles are efficiently internalized and released in PC3 cells.

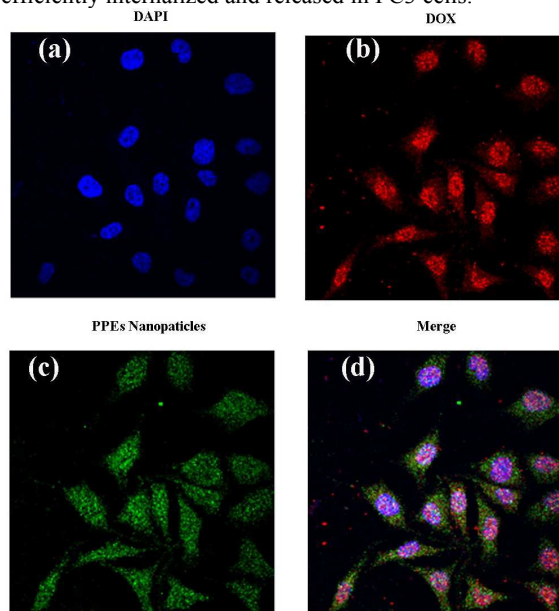


Figure 8 Confocal microscopy images of PC3 cells after incubation with DOX loaded PPE nanoparticles for 12 h. For each panel, images from (a) were cells with nuclear staining with DAPI (blue), (b) cells with PPEs

nanoparticles (green), (c), cells with DOX (red), (d) overlays of blue, green and red fluorescence channels.

Efficacy of DOX Loaded PPEs Nanoparticles in Killing PC3 Cells

In addition, the growth inhibition test of PC3 cells was carried out to evaluate the antitumor activity of DOX loaded PPEs nanoparticles and free DOX. As shown in Figure 9, the cell viabilities decrease with increasing DOX concentrations and DOX loaded PPEs nanoparticles exhibited lower cytotoxicity to PC3 cells compared with free DOX at the same dosages, which may be resulted from the prolonged release of DOX from PPEs nanoparticles. It should be noted that the IC₅₀ of DOX loaded PPEs nanoparticles (4.23 μg/mL) is higher than that of free DOX (1.71 μg/mL) in PC3 cells. These results suggested that PPEs nanoparticles could maintain the drug activity to effectively inhibit the growth of cancer cells and reduce the toxicity of drug.

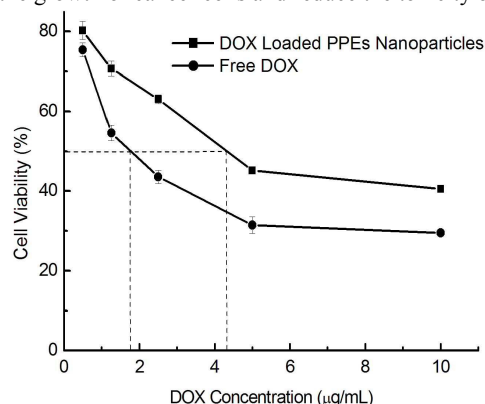


Figure 9 In vitro cytotoxicity of DOX loaded PPEs nanoparticles and free DOX in PC3 cells.

PPEs Nanoparticles Mediated DOX Delivery System Strengthens Cell Apoptosis in PC3 Cells

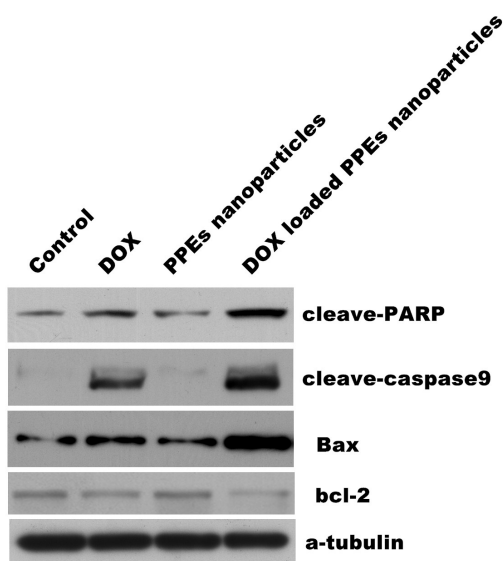


Figure 10 Western blots of the PC3 cells. The lanes were loaded with PBS as control sample, DOX, PPEs nanoparticles, and DOX loaded PPEs nanoparticles. DOX is most widely used in the treatment of solid tumor,¹³ the mitochondria dependent apoptotic pathway was believed the

main mechanism underlying DOX-induced apoptosis,¹⁴ accompanied by a significant upregulation of the Bax and cleave-caspase9 expression and down regulation of the BCL-2 expression (Figure 10). In addition, PARP is a protein involved in many cellular processes as DNA repair and cell apoptosis, and cleaved PARP, a marker of apoptosis, increased in DOX induced apoptosis. The western blot analysis was also performed to evaluate the antitumor activity of DOX loaded PPEs nanoparticles. As shown in Figure 10, comparing with control, DOX loaded PPEs nanoparticles caused a marked increase in cleavage PARP and apoptotic proteins, including cleave-caspase9 and Bax, while the anti-apoptotic protein Bcl-2 were strongly blocked, drastically leading to apoptotic cell death. Next we tried to determine the influence of PPEs nanoparticles on apoptosis of PC3 cells. As exhibited in Figure 10, no significant change in expression of indicated proteins compared to control, which is consisted with the results above from CCK-8. Taken together, the present results implied that PPEs nanoparticles delivery system could deliver DOX into cells and efficiently result in cell apoptosis.

Conclusions

In summary, a novel amphiphilic poly(phenyleneethynylene)s has been designed and synthesized. The amphiphilic poly(phenyleneethynylene)s could self assemble into nanoparticles, named PPEs nanoparticles. The morphology of PPEs nanoparticles was investigated. *In vitro* cell viability assay showed that PPEs nanoparticles exhibited good biocompatibility and low toxicity. Moreover, confocal laser scanning microscopy and flow cytometry assay revealed the effective internalization of PPEs nanoparticles in PC3 cells. This suggests that PPEs nanoparticles can be used as cell imaging agent.

Furthermore, the potential of PPEs nanoparticles for use as a drug carrier was also investigated using DOX as a model hydrophobic therapeutic drug. DOX loaded PPEs nanoparticles were characterized and drug release behaviour was evaluated. The study by live cell imaging system further revealed that DOX loaded PPEs nanoparticles successfully entered into cells and DOX was efficiently released. More importantly, cytotoxicity and cell apoptosis in PC3 cells illustrated that DOX loaded PPEs nanoparticles exhibit higher therapeutic efficiency than free DOX. All the results demonstrated that the delivery systems based on PPEs nanoparticles would be a promising platform for therapeutic delivery and/or bioimaging applications.

Acknowledgements

We gratefully thank the "Medical Scientific Research Foundation of Guangdong Province, China (A2010355)" for financial support of this work.

Notes and references

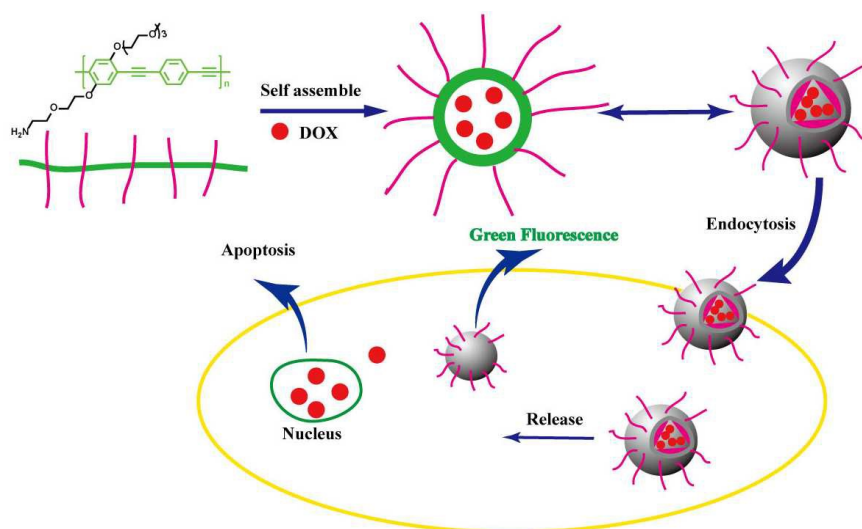
- ^a School of Pharmaceutical Sciences, Southern Medical University, Guangzhou 510515, China. *Corresponding author. Tel: 86202061648196; E-mail: ruiyiliu@smu.edu.cn
- ^b Department of Urology, Nan Fang Hospital, Southern Medical University, Guangzhou 510515, China.
- ^c Department of Cell Biology, School of Basic Medical Sciences, Southern Medical University, Guangzhou 510515, China. *Corresponding author. E-mail: Zhyke@smu.edu.cn

† Electronic Supplementary Information (ESI) available: [details of any supplementary information available should be included here]. See DOI: 10.1039/b000000x/

‡ These two authors contributed equally to this work.

- 1 G. Orive, R.M. Hernandez, G. A. Rodriguez, A. Dominguez-Gil, and J. L. Pedraz, *Curr Opin Biotechnol.* 2003, **14**, 659; R. V. J. Chari, *Acc. Chem. Res.*, 2008, **41**, 98.
- 2 R. Duncan, *Nat. Rev. Drug Discovery*, 2003, **2**, 347; R. Duncan, *Nat. Rev. Drug Discovery* 2003, **2**, 347; A. V. Kabanov, *Adv. Drug Delivery Rev.* 2006, **58**, 1597; V. P. Torchilin, *Pharm. Res.*, 2007, **24**, 1; J. Fang, H. Nakamura, and H. Maeda, *Adv. Drug Delivery Rev.* 2011, **63**, 136.
- 3 D.D. Guo, H.S. Moon, R. Arote, J.H. Seo, J.S. Quan, Y.J. Choi and C.S. Cho, *Cancer Lett.*, 2007, **254**, 244; K. Miyata, L. J. Wong, C. Boyer, Z. F. Jia, H. M. Zareie, T. P. Davis, V. Bulmus, *Biomacromolecules* 2008, **9**, 1934; Y. F. Zhou, W. Huang, J. Y. Liu, X. Y. Zhu, and D. Y. Yan, *Adv. Mater.* 2010, **22**, 4567; S. Shu, C. Sun, X. Zhang, Z. Wu, Z. Wang, C. Li, *Acta Biomater.* 2010, **6**, 210; J. Wen, S. M. Anderson, J. Du, M. Yan, J. Wang, M. Shen, Y. Lu, T. Segura, *Adv. Mater.* 2011, **23**, 4549; M. X. Zhao, A. Biswas, B. L. Hu, K. I. Joo, P. Wang, Z. Gu, Y. Tang, *Biomaterials* 2011, **32**, 5223; Y. Wang, C. Y. Hong, and C. Y. Pan, *Biomacromolecules* 2013, **14**, 1444; L. Mazzarino, I. Otsuka, S. Halila, L. S. Bubniak, S. Mazzucco, M. C. Santos-Silva, E. Lemos-Senna, and R. Borsali *Macromol. Biosci.* 2014, **14**, 709.
- 4 R. Weissleder, and V. Ntziachristos, *Nat. Med.* 2003, **9**, 123; A. M. Smith, H. Duan, A. M. Mohs, and S. Nie, *Adv. Drug Delivery Rev.* 2008, **60**, 1226; X. Feng, L. Liu, S. Wang, and D. Zhu, *Chem. Soc. Rev.* 2010, **39**, 2411.
- 5 H. S. Choi, W. Liu, P. Misra, E. Tanaka, J. P. Zimmer, B. I. Ipe, M. G. Bawendi, and J. V. Frangioni, *Nat. Biotechnol.* 2007, **25**, 1165; M. De, P. S. Ghosh and V. M. Rotello, *Adv. Mater.*, 2008, **20**, 4225; Y. Su, M. Hu, C. Fan, Y. He, Q. Li, W. Li, L.-h. Wang, P. Shen and Q. Huang, *Biomaterials*, 2010, **31**, 4829; V. Biju, T. Itoh, and M. Ishikawa *Chem. Soc. Rev.* 2010, **39**, 3031; P. Zrazhevskiy, M. Sena and X. Gao, *Chem. Soc. Rev.*, 2010, **39**, 4326; Y. P. Ho, K. W. Leong, *Nanoscale* 2010, **2**, 60; K. Lee, J. Lee, E. J. Jeong, A. Kronk, K. S. J. Elenitoba-Johnson, M. S. Lim, and J. Kim, *Adv. Mater.* 2012, **24**, 2479; P. Wu, and X.P. Yan *Chem. Soc. Rev.* 2013, **42**, 5489.
- 6 J. M. Tour, *Chem. Rev.*, 1996, **96**, 537; J. S. Moore, *Chem. Rev.*, 1997, **30**, 402; U. H. F. Bunz, *Chem. Rev.*, 2000, **100**, 1605; Swager, T. M. *Acc. Chem. Res.* 1998, **31**, 201; D. T. McQuade, A. E. Pullen, T. M. Swager, *Chem. Rev.*, 2000, **100**, 2537.
- 7 J. Kim, D. T. McQuade, S. K. McHugh, T. M. Swager, *Angew. Chem., Int. Ed.*, 2000, **39**, 3868; Z. Chen, C. Xue, W. Shi, F.-T. Luo, S. Green, J. Chen, H. Liu, *Anal. Chem.*, 2004, **76**, 6513; I.B. Kim, B. Erdogan, J. N. Wilson, U. H. F. Bunz, *Chem. Eur. J.*, 2004, **10**, 6247; I.B. Kim, A. Dunkhorst, J. Gilbert, U. H. F. Bunz, *Macromolecules*, 2005, **38**, 4560; Q. L. Fan, Y. Zhou, X.M. Lu, X.Y. Hou, W. Huang, *Macromolecules*, 2005, **38**, 2927; X. Zhao, Y. Liu, K. S. Schanze, *Chem. Commun.*, 2007, 2914; X. Yong, W. Wan, M.G. Su, W.W. You, X.W. Lu, Y.C. Yan, J.Q. Qu, R.Y. Liu and T. Masuda, *Polym. Chem.*, 2013, **4**, 4126; W.F. Zeng, X.D. Yang, X.L. Chen, Y.C. Yan, X.W. Lu, J.Q. Qu, and R.Y. Liu, *Eur. Polym. J.* 2014, **61**, 309; W.F. Zeng, X. Yong, X.D. Yang, Y.C. Yan, X.W. Lu, J.Q. Qu, and R.Y. Liu, *Macromol. Chem. Phys.* 2014, **215**, 1370.
- 8 D. Pan, J. L. Turner and K. L. Wooley, *Chem. Commun.*, 2003, 2400; I-B. Kim, H. Shin, A. J. Garcia and U. H. F. Bunz, *Bioconjugate Chem.*, 2007, **18**, 815; J. H. Moon, E. Mendez, Y. Kim and A. Kaur, *Chem. Commun.*, 2011, 8370; C. L. Zhu, L. B. Liu, Q. Yang, F. T. Lv, S. Wang, *Chem. Rev.* 2012, **112**, 4687; T. Vokata and J. H. Moon, *Macromolecules*, 2013, **46**, 1253; C. Yin, W. Song, R. Jiang, X. Lu, W. Hu, Q. Shen, X. Li, J. Li, Q. Fan and W. Huang *Polym. Chem.*, 2014, **5**, 5598.
- 9 T. Zhang, H. Fan, J. Zhou, G. Liu, G. Feng, and Q. Jin, *Macromolecules* 2006, **39**, 7839.
- 10 R. B. Prince, J. G. Saven, P. G. Wolynes, and J. S. Moore, *J. Am. Chem. Soc.* 1999, **121**, 3114.
- 11 N. A. A. Rahim, W. McDaniel, K. Bardou, S. Srinivasan, V. Vickerman, P. T. C. So and J. H. Moon, *Adv. Mater.*, 2009, **21**, 3492.
- 12 J. Xu, Q. Zhao, Y. Jin and L. Qiu, *Nanomedicine: Nanotechnology, Biology, and Medicine*, 2014, **10**, 349.
- 13 G. Takemura and H. Fujiwara, *Prog. Cardiovasc. Dis.* 2007, **49**, 330; W.T. Chang, J. Li, H.H. Haung, H. Liu, M. Han, S. Ramachandran, C.Q. Li, W.W. Sharp, K.J. Hamann, C.S. Yuan, T.L. Hoek and Z.H. Shao, *J. Cell Biochem.* 2011, **112**, 2873.
- 14 J. Sun, G. Sun, X. Meng, H. Wang, Y. Luo, M. Qin, B. Ma, M. Wang, D. Cai, P. Guo and X. Sun, *PLoS One.* 2013, **8**, e64526.

Graphical Contents



A novel PPEs nanoparticles self-assembled from amphiphilic poly(phenyleneethynylene) would be a promising drug delivery system for therapeutic delivery and/or bioimaging.